NeuroImage: Clinical 4 (2014) 757–764

Contents lists available at ScienceDirect

NeuroImage: Clinical

journal homepage: www.elsevier.com/locate/ynicl

Individual classification of children with epilepsy using support vector machine with multiple indices of diffusion tensor imaging

Ishmael Amarreh [a,*], Mary E. Meyerand [a], Carl Stafstrom [b], Bruce P. Hermann [b], Rasmus M. Birn [a,c]

[a] Department of Medical Physics, University of Wisconsin School of Medicine and Public Health Madison, WI 53705, United States
[b] Department of Neurology, University of Wisconsin School of Medicine and Public Health Madison, WI 53705, United States
[c] Department of Psychiatry, University of Wisconsin-Madison, United States

ARTICLE INFO

Article history:
Received 23 December 2013
Received in revised form 13 February 2014
Accepted 14 February 2014
Available online 29 March 2014

Keywords:
DTI
Childhood epilepsy
Remission
Support vector machine

ABSTRACT

Introduction: Support vector machines (SVM) have recently been demonstrated to be useful for voxel-based MR image classification. In the present study we sought to evaluate whether this method is feasible in the classification of childhood epilepsy intractability based on diffusion tensor imaging (DTI), with adequate accuracy. We applied SVM in conjunction DTI indices of fractional anisotropy (FA), mean diffusivity (MD), radial diffusivity (RD) and axial diffusivity (AD). DTI studies have reported white matter abnormalities in childhood-onset epilepsy, but the mechanisms underlying these abnormalities are not well understood. The aim of this study was to examine the relationship between epileptic seizures and cerebral white matter abnormalities identified by DTI in children with active compared to remitted epilepsy utilizing an automated and unsupervised classification method.

Methods: The DTI data were tensor-derived indices including FA, MD, AD and RD in 49 participants including 20 children with epilepsy 5–6 years after seizure onset as compared to healthy controls. To determine whether there was normalization of white matter diffusion behavior following cessation of seizures and treatment, the epilepsy subjects were grouped into those with active versus remitted epilepsy. Group comparisons were previously made examining FA, MD and RD via whole-brain tract-based spatial statistics (TBSS). The SVM analysis was undertaken with the WEKA software package with 10-fold cross validation. Weighted sensitivity, specificity and accuracy were measured for all the DTI indices for two classifications: (1) controls vs. all children with epilepsy and (2) controls vs. children with remitted epilepsy vs. children with active epilepsy.

Results: Using TBSS, significant differences were identified between controls and all children with epilepsy, between controls and children with active epilepsy, and also between the active and remitted epilepsy groups. There were no significant differences between the remitted epilepsy and controls on any DTI measure. In the SVM analysis, the best predictor between controls and all children with epilepsy was MD, with a sensitivity of 90–100% and a specificity between 96.6 and 100%. For the three-way classification, the best results were for FA with 100% sensitivity and specificity.

Conclusion: DTI-based SVM classification appears promising for distinguishing children with active epilepsy from either those with remitted epilepsy or controls, and the question that arises is whether it will prove useful as a prognostic index of seizure remission. While SVM can correctly identify children with active epilepsy from other groups' diagnosis, further research is needed to determine the efficacy of SVM as a prognostic tool in longitudinal clinical studies.

1. Introduction

Diffusion tensor imaging in childhood epilepsy has improved our understanding of the impact of epilepsy on brain structure. Children with mixed new-onset epilepsy syndromes have been shown to exhibit reduced fractional anisotropy (FA) and increased radial diffusivity (RD) in the posterior corpus callosum and cingulum (Hutchinson et al., 2010), as well as significantly higher FA and lower MD, AD and RD in the internal capsule, cingulum, body of the corpus callosum, superior corona radiata and superior fronto-occipital fasciculus (Amarreh et al., 2013). Reduced FA in the anterior limbs of the internal capsule (AIC), the posterior limbs of the internal capsule (PIC), and the splenium of the corpus callosum (SCC) and higher MD, RD and axial diffusivity (AD) were reported in the AIC, PIC and SCC in adolescents and children with epilepsy (Meng et al., 2010). Additionally, DTI results from

* Corresponding author at: Department of Medical Physics, University of Wisconsin School of Medicine and Public Health, 1005 Wisconsin Institutes for Medical Research (WIMR), 1111 Highland Avenue, Madison, WI 53705, United States.
E-mail address: amarreh@wisc.edu (I. Amarreh).

http://dx.doi.org/10.1016/j.nicl.2014.02.006

pediatric temporal lobe epilepsy studies include significantly reduced FA in the hippocampus contralateral as well as ipsilateral to the side of seizure onset (Kimiwada et al., 2006) and decreased anisotropy in white matter tracts (uncinate, arcuate, and inferior longitudinal fasciculus as well as corticospinal tract) both contralateral as well as ipsilateral to the side of seizure onset (Govindan et al., 2008). These white matter abnormalities have been reported in regions both near to as well as distant from the primary epileptic zone (Arfanakis et al., 2002; Concha et al., 2009; Diehl et al., 2008; Knake et al., 2009; Rodrigo et al., 2007; Thivard et al., 2005).

In addition to DTI, maps of functional activation and connectivity, measured by neuroimaging modalities such as task-based fMRI and resting state functional MRI (rsfMRI) respectively, have shown that epilepsy is associated not only with structural but also with functional brain changes, further improving our understanding of the neurobiology of epilepsy (Arfanakis et al., 2002; Duncan, 2002, 2008; Hermann et al., 2006; Obenaus and Jacobs, 2007). To date, differences in structural and functional images have been used mainly to characterize disparities between groups, i.e., controls vs. epilepsy groups. Unfortunately, group-based methods are not helpful in inferring specific clinical outcomes for an individual patient. Therefore, and for the purpose of individual discrimination, a desirable method would be one that can compare a single subject's scans to a group of healthy controls. Machine learning (ML) algorithms, such as support vector machine (SVM) pattern recognition algorithm, fulfills this requirement.

In epilepsy, the use of machine learning algorithms has been primarily for seizure detection. SVM classifiers have been applied to discriminate between seizure and non-seizure EEG epochs in newborns with seizures secondary to hypoxic ischemic encephalopathy (Temko et al., 2011). Also, SVM classifiers have been used to identify the onset of seizures in non-invasive EEG from pediatric subjects suffering from a variety of seizure types (Shoeb et al., 2004). Recently in a study of temporal lobe epilepsy using SVM, DTI indices were reported to have diagnostic advantage over other T-1 based classification (Focke et al., 2012). To the best of our knowledge, the present study is among the first to examine SVM as a tool for classifying seizure outcomes in children with epilepsy (remitted versus persisting seizures).

2. Methods and materials

We previously conducted a cross-sectional analysis of DTI measures in children with epilepsy vs. healthy controls 5–6 years after seizure onset (Amarreh et al., 2013), examining differences between the control and epilepsy groups overall as well as by epilepsy status (active versus remitted epilepsy), using tract based spatial statistics (TBSS) pipeline within FSL (Smith et al., 2006). Of special interest were comparisons within the epilepsy group categorized into groups based on their seizure outcomes (active, remitted) and compared to controls. Here we utilize DTI measures from the TBSS pipeline with SVM, our goal being to evaluate the feasibility of individual classification of children with epilepsy.

2.1. Subject groups

Participants were 49 children and adolescents (aged 8–18 years at the recent onset of epilepsy) including 20 participants with epilepsy (9 females, 11 males) and 29 normally developing participants (median age = 18 years; 13 females, 16 males). The epilepsy participants were selected based on a diagnosis of idiopathic epilepsy with no other developmental disabilities or neurological disorders and normal brain MRI scans. The epilepsy group contained 9 with active epilepsy (median age = 19 years; 5 females, 4 males) and 11 with remitted epilepsy (median age = 16 years; 4 females, 7 males). Epilepsy remission was defined as remaining seizure free for 12 months and no longer taking anti-epileptic drugs (AEDs). Children with localization-related (n = 6) and generalized epilepsy (n = 5) were equally represented in the remitted group. The 29 control participants were first-degree cousins of the children with epilepsy who were comparable in age, gender and handedness to the epilepsy group (Table 1). The control group had no history of seizures and no other developmental or neurological diseases. The full details on the selection criteria are available elsewhere (Hermann et al., 2006). The results presented here involve DTI scans taken at the third visit—5-6 years after their baseline evaluation. A total of 84 DTI scans were collected, but due to a scanner malfunction, 32 scans contained image artifacts and were not included in this analysis, leaving a final sample size of 23 epilepsy participants and 29 controls. Three epilepsy subjects could not be confidently classified as active or remitted and thus were not included in the analysis. This study was reviewed and approved by the Institutional Review Boards of both institutions. On the day of study participation families and children gave informed consent and assent and all procedures were consistent with the Declaration of World Medical Organization (1996).

2.2. Image acquisition

T1, T2, and diffusion weighted (DWI) MRIs' were acquired for each participant. All MRI scans were collected on a clinical 1.5 T GE Signa LX MRI scanner (General Electric Corporation, Milwaukee, WI). T1-weighted, Axial Bravo stealth scans are collected with TR/TE = 10.6/4.36 ms, flip angle = 13°, axial acquisition with a reconstructed matrix size of 512 × 512, field of view (FOV) = 162 mm, slice thickness 1.5 mm and contiguous spacing. DTI scan parameters are as follows: one reference scan with b = 0 s/mm^2 and 25 diffusion weighted scans with b = 1000 s/mm^2 each with a unique set of gradient directions optimized for DTI axial acquisition with a reconstructed matrix size of 256 × 256, FOV = 120 mm, and slice thickness = 3 mm.

2.3. DTI analysis

Images were transferred to an offline workstation for processing. After initial conversion of the imaging data to the NIFTI format, preprocessing was performed with the FMRIB Software Tools (FSL) software

Table 1
Demographic characteristics of the epilepsy and control groups.

	Epilepsy (n = 20)	Control (n = 29)	Median
	Remit (n = 11)	Active (n = 9)	
	Median	Median	
Age (years)	16	19	18
Gender	7 M/4 F	4 M/5 F	16 M/13 F
IQ full score*	120.27 (9.50)*	107.00 (8.12)*^	117.14 (10.63)^
Seizure duration (years)	6.81 (0.72)*	5.90 (0.70)*	–
Age of onset (years)	11.53 (3.20)	11.95 (3.52)	
Syndrome	6 ILRE/5 IGE	7 ILRE/2 IGE	
Antiepileptic drugs (polytherapy, monotherapy, none)	0/0/11*	4/4/1*	–

Superscript symbol pairs ("*", "^") denote significant differences; $p < 0.05$. ILRE = idiopathic localization-related epilepsy; IGE = Idiopathic generalized epilepsy.

package unless otherwise indicated (Woolrich et al., 2009). The FSL eddy current correction toolbox was used to correct for eddy-current artifacts. Computation of the diffusion tensor and the relevant tensor-derived indices were performed with the HI-SPEED software packets (https://sites.google.com/site/hispeedpackets/), which uses a constrained nonlinear least squares method for estimating the diffusion tensor (Koay et al., 2006). These maps were then used in the voxel-wise analyses to disambiguate differences in specific structures of brain white matter. To address the structural differences in white matter, we conducted a voxel-wise analysis using white matter skeleton of DTI indices of FA, MD, RD and AD generated by TBSS (Fig. 1) (Smith et al., 2006). The full details of TBSS processing are available elsewhere (Amarreh et al., 2013).

2.4. SVM

Machine-learning (ML) techniques have been applied to a range of MRI methods in an effort to automate the diagnosis of different brain disorders. This includes the use of volumetric analysis of the hippocampus combined with logistic regression in individuals with mild cognitive impairment and Alzheimer's disease (Desikan et al., 2009), as well as the combination of support vector machine (SVM) with gray matter (GM) data from voxel based morphometry (VBM) to classify Alzheimer patients (Klöppel et al., 2008; Magnin et al., 2009). A combination of structural MRI with PET data has been found to increase accuracy when using SVM (Fan et al., 2008).

In what follows, we provide an overview of SVM and its application to brain imaging data. SVM is a specific type of supervised ML method that learns how to assign labels to objects (Noble, 2006; Vapnik and Lerner, 1963). These algorithms classify input data into separable clusters or "classes" based on defined attributes, which in ML are generally known as "features". The main steps of the SVM method comprise (i) preparing data for input into classifier training, (ii) training and testing the classifier, and (iii) evaluating its performance.

2.4.1. Preparing data for classifier training

The first step of developing a classifier involves two procedures: "feature extraction" and "feature selection". The first of these two procedures, feature extraction, involves the transformation of the original data into a set of "features" which can be used as input data into SVM. By comparison, feature selection, as the name implies, is a data reduction method, which involves the selection of a subset of features that will facilitate learning. In neuroimaging, the rational for feature selection is threefold. Firstly, reducing features helps the accuracy of the classifier. Secondly, reducing the number of features helps localize the discriminative regions between the groups, which aids in neuroscience interpretations. Thirdly, removing redundant features speeds up the computational time (Orrù et al., 2012).

2.4.2. Training and testing the classifier

In the second step, SVM is trained using data predefined into experimentally set groups of interest (e.g. controls and patients) to estimate a mathematical rule or "decision function", which best distinguishes between the groups or "classes". Fig. 2 illustrates a hypothetical classification problem between subjects (red circles) and controls (blue circles) for the simplified case of two cerebral voxels. Each axis represents the measurement in one voxel, with each symbol (colored circles) representing a brain scan of a different individual. In this two-dimension example there are a number of possible ways one can delineate between the groups as presented by straight lines (see Fig. 2a). In SVM, an algorithm is trained that provides the best line or "classifier" that separates the two groups. The algorithm achieves this by adopting the line that gives the greatest separation between the two groups based on the measurements closest to the line, otherwise known as support vectors (see Fig. 2b).

While in a two-dimension space a straight line can separate the space in half (Fig. 2b), in three dimensions, we need a plane to divide the space. The general term used for a straight line in a high dimension space is hyperplane, and thus a separating hyperplane is essentially a line separating classes in a high dimension space. The line that gives the maximum separation between classes is called the maximum margin hyperplane and the closest instances to the hyperplane are called the support vectors (Fig. 2b). The projection of the data from a low dimensional space to a higher dimensional space is achieved with a kernel function. The optimal kernel function is usually found by trial and error. In the current study a radial basis function (RBF) kernel was used to nonlinearly map samples into a higher dimensional space. RBF kernels use two parameters: C and GAMMA. GAMMA represents the width of the radial basis function, and C represents the error/trade-off parameter that adjusts the importance of the separation error in the creation of the separation surface. Therefore, SVM is a specific type of supervised ML method that aims to classify data points by maximizing the margin hyperplane (Lemm et al., 2011).

In the testing phase, once the SVM algorithm has been trained, it is used to predict the group to which a new and previously unseen subject belongs. The prediction is based on the distance between the subject

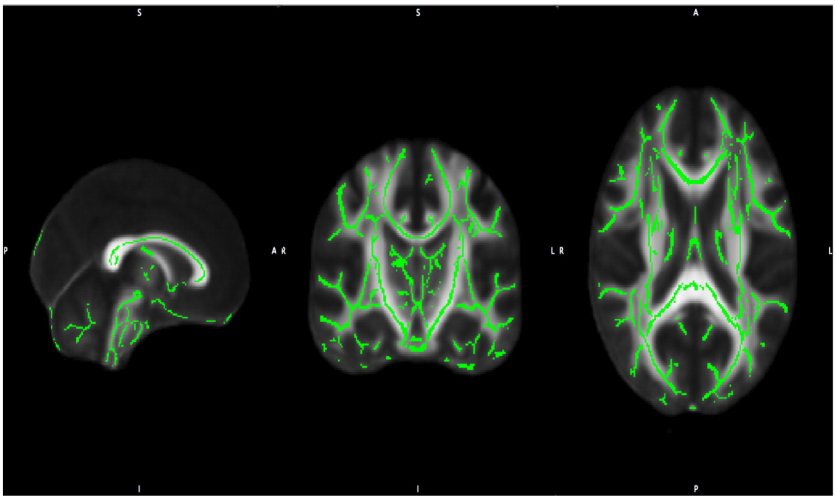

Fig. 1. Three views of the mean FA skeleton superimposed on the standard FMRIB template. The skeleton is thresholded at 0.2 and demonstrates good alignment with minimal signal intensity in the outer brain.

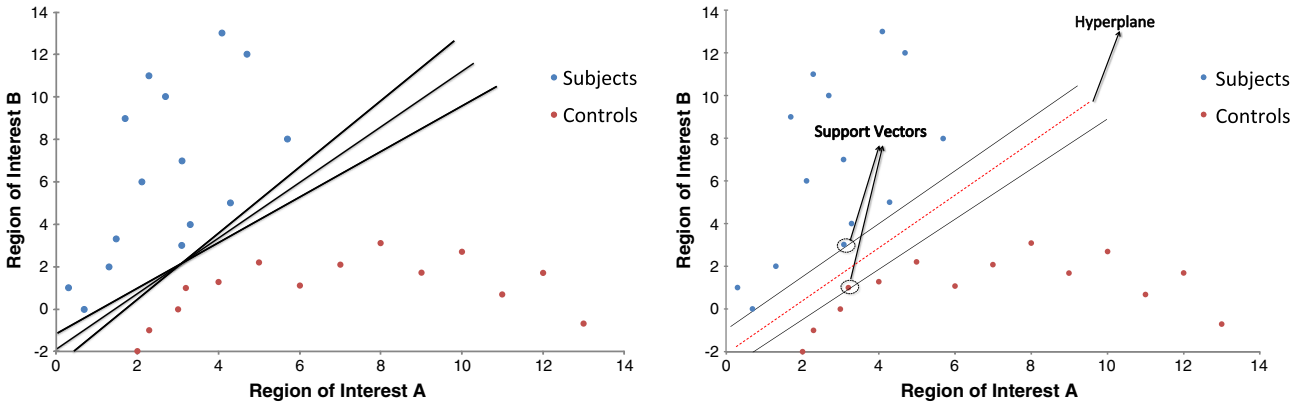

Fig. 2. Hypothetical pattern classification problem between subjects (red circles) and controls (blue circles). Each symbol (circle) represents the brain scan of a different subject. (a) Using different pattern classification methods, it is possible to obtain several different classifiers that correctly separate the two groups; these are represented by lines. (b) Using SVM, an optimal classifier is obtained as represented by the red dashed line and the support vectors are represented by arrow symbols.
Reproduced with permission (Orrù et al., 2012).

and the separating hyperplane; in our study this distance was used to determine, via Platt's "sequential minimal optimization" (SMO) method (Platt, 1998), the probabilistic score for the subject and the subject is labeled based on the sign of the score (O'Dwyer et al., 2012). The SMO is capable of handling multi-class problems using pairwise classification (Trevor and Robert, 1998). In the 10-fold cross-validation used in this analysis, the original sample is randomly partitioned into 10 subsamples. Of the 10 subsamples, a single subsample is retained as the validation data for testing the model, and the remaining 9 subsamples are used as training data. The cross-validation process is then repeated 10 times (the folds), with each of the 10 subsamples used exactly once as the validation data. The 10 results from the folds can then be averaged to produce a single estimation. This is a standard procedure in machine learning, which reduces the variation related to data selection, and allows the results to be averaged to yield a robust calculation of the performance of the SVM.

2.4.3. Classifier evaluation

In the analysis of the results, the performance of a classifier can be measured by its sensitivity, specificity and accuracy. Sensitivity, which is the ability of the classifier to correctly identify positive results, is defined as TP/(TP + FN) and specificity refers to the ability to correctly identify negative results and is defined as TN/(FP + TN). Accuracy is defined as (TP + TN)/(TP + TN + FN + FP).

2.5. SVM analysis

In this study the individual classification was undertaken using the open source WEKA software package (http://www.cs.waikato.ac.nz/ml/weka/, version 3.6.8). Following the TBSS preprocessing the skeletonized FA, MD, RD and AD data was analyzed in Matlab program, which extracted and transformed the diffusion data into a WEKA compatible format. Analysis was carried out for the classification of: 1) controls and children with epilepsy and 2) controls and children with active or remitted epilepsy.

The first step of the WEKA classification was data reduction. Utilizing the feature selection algorithm "ReliefF" (Robnik-Šikonja and Kononenko, 2003) the number of voxels was reduced to the most relevant for classification. Five different data reductions were evaluated, which reduced the full FA, MD, RD and AD from approximately 130,000 voxels into reduced data sets of 250, 500, 1000, 2000, and 3000 voxels. The voxels from these reduced data sets are our features in this classification analysis.

In the second step, the three groups were classified by using the SVM algorithm "sequential minimal optimization" SMO (Platt, 1998) with radial basis function with C fixed to 1 and GAMMA fixed to 0.01 (Scholkopf et al., 1997). In our analysis, the classifier was evaluated via the 10-fold cross validation to ensure performance generalization. The results of the accuracy are the average of 10 repetitions of 10-fold cross validations, while sensitivity and specificity values are of a single repetition of 10-fold cross validations. In the multi-classification of the controls vs. the active and the remitted epilepsy, the 3 groups were paired-wise compared in 3 distinct SVM analyses.

3. Results

3.1. TBSS group differences

Below we present a brief summary of the results of the prior TBSS analysis (Amarreh et al., 2013).

Examining the total epilepsy versus control groups, the participants with epilepsy showed reduced FA in major white matter tracts (Fig. 3) with an increase in MD, AD and RD in the epilepsy group compared to controls. Of note is that MD and AD had the most regions that showed differences between these groups (Amarreh et al., 2013).

When the epilepsy group was divided into those with active versus remitted seizures, there were no differences in any of the DTI indices between the remitted epilepsy group and controls. In contrast, the active epilepsy group showed reduced FA in several brain regions compared to controls. This active epilepsy group also exhibited an increase in MD, RD and AD. Of note is that FA had the most regions that showed differences between controls and children with active epilepsy (Supplemental file Table 1) (Amarreh et al., 2013).

When the active group and remitted group were compared, the active epilepsy group showed reduced FA and increased MD, RD and AD. Of note is that FA and RD had the most regions that showed differences between controls and children with active epilepsy (Supplemental file Table 2) (Amarreh et al., 2013).

3.2. SVM classification

3.2.1. Controls and children with epilepsy

In line with the aforementioned TBSS results, the highest classification was achieved with MD and AD. Sensitivity for MD ranged from 90 to 100% and specificity ranged from 96.6 to 100% for the tested data set. Sensitivity for AD was 98.1% for all subsets of the tested data while specificity was 100%. For FA and RD, classification performance had a sensitivity and a specificity in the range of 90–96.6% (Fig. 4). In this classification, the peak of the classification performance was reached with MD and AD.

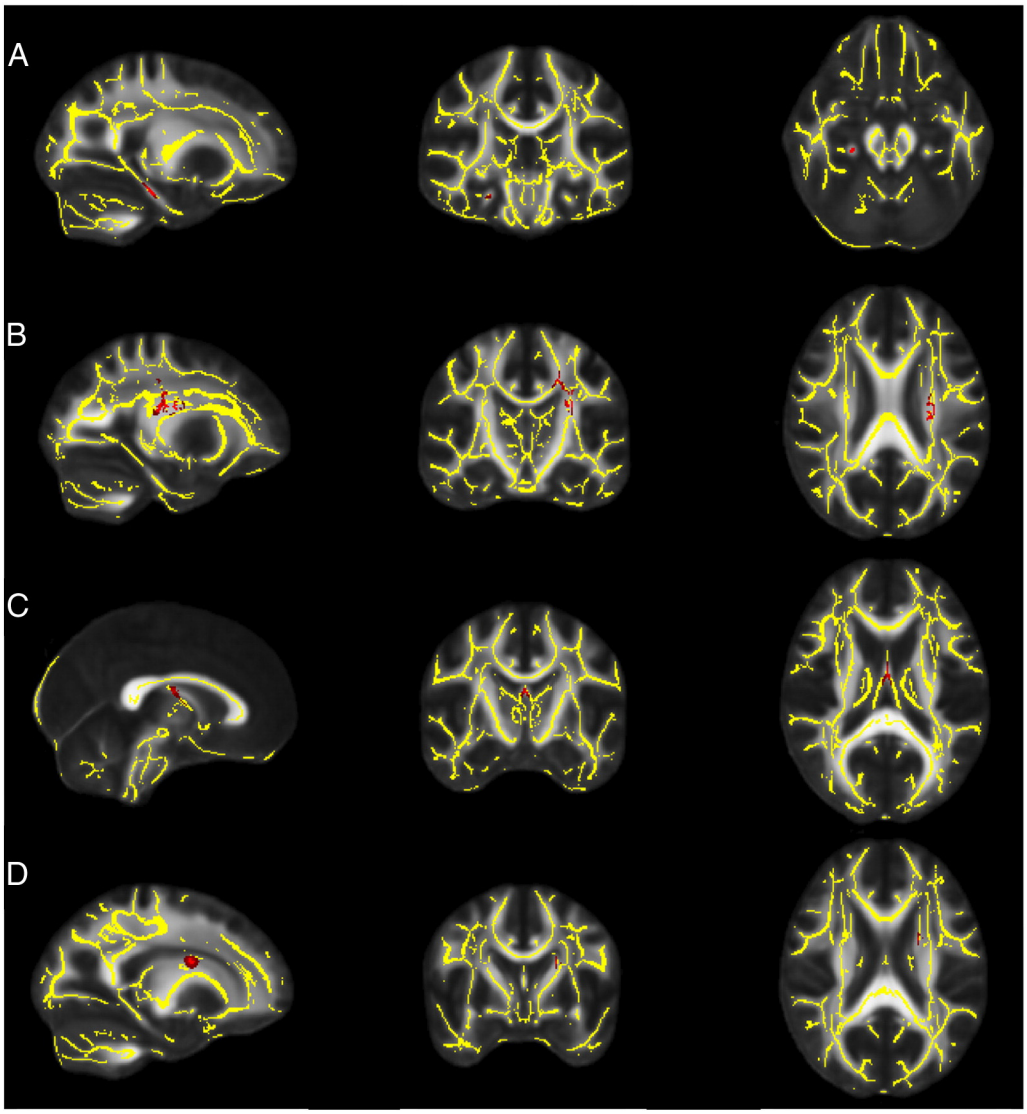

Fig. 3. Representative regions that were significantly abnormal in children with epilepsy (n = 20) compared to controls (n = 29) after multiple corrections. Gray is the standard FA template; overlaid is the white matter skeleton (yellow). (A) The right cingulate cortex with lower FA in children with epilepsy compared to controls (red). (B–D) Left superior corona radiata, fornix and the left superior fronto-occipital fasciculus with higher MD, RD and AD respectively in children with epilepsy (red).
Reproduced with permission (Amarreh et al., 2013).

3.2.2. Controls and children with active epilepsy versus remitted epilepsy

Across the reduced data sets of DTI metrics evaluated, the best classification results were achieved using FA at 500 voxels with 100% sensitivity and specificity. In the TBSS results the number of regions was highest in the FA analysis between controls and children with active epilepsy. The second highest classification was achieved using AD at 500 voxels with 98% sensitivity and specificity. In the TBSS results the number of regions was highest in the AD analysis between children with active epilepsy and children with remitted epilepsy For MD and RD, classification performance was in the range of 65–95% sensitivity and specificity (Fig. 5).

4. Discussion

The primary finding of this preliminary study is that individual classification using automated SVM of DTI data in childhood epilepsy is feasible with a high degree of accuracy. The SVM results are also in broad agreement with results from the TBSS analysis previously reported (Amarreh et al., 2013). All the classification results achieved high accuracies (90% range) in the controls vs. all epilepsy patients with MD being the measure with the best ability to classify patients. In the TBSS analysis the largest number of regions that showed differences between controls and the entire epilepsy group were in MD and AD maps. Interestingly, a recent machine learning study in temporal lobe epilepsy also indicated that the MD index was the optimal index for epilepsy and control classification (Focke et al., 2012).

When the classification was extended to three-groups including controls, children with active and children with remitted epilepsy, the FA features achieved 100% accuracy in classification between controls vs. children with active epilepsy vs. children with remitted epilepsy. This pattern was also observed in the TBSS results where differences in FA were exhibited in more regions than the other DTI indices.

4.1. Clinical implication of SVM in the prediction of seizure intractability

Factors predicting seizure remission have been studied extensively from a clinical viewpoint and results have been variable across studies. Several studies have identified clinical factors such as age of seizure onset, seizure frequency, seizure type, EEG findings, response to initial therapy, and epilepsy syndrome (e.g., genetic generalized epilepsy or

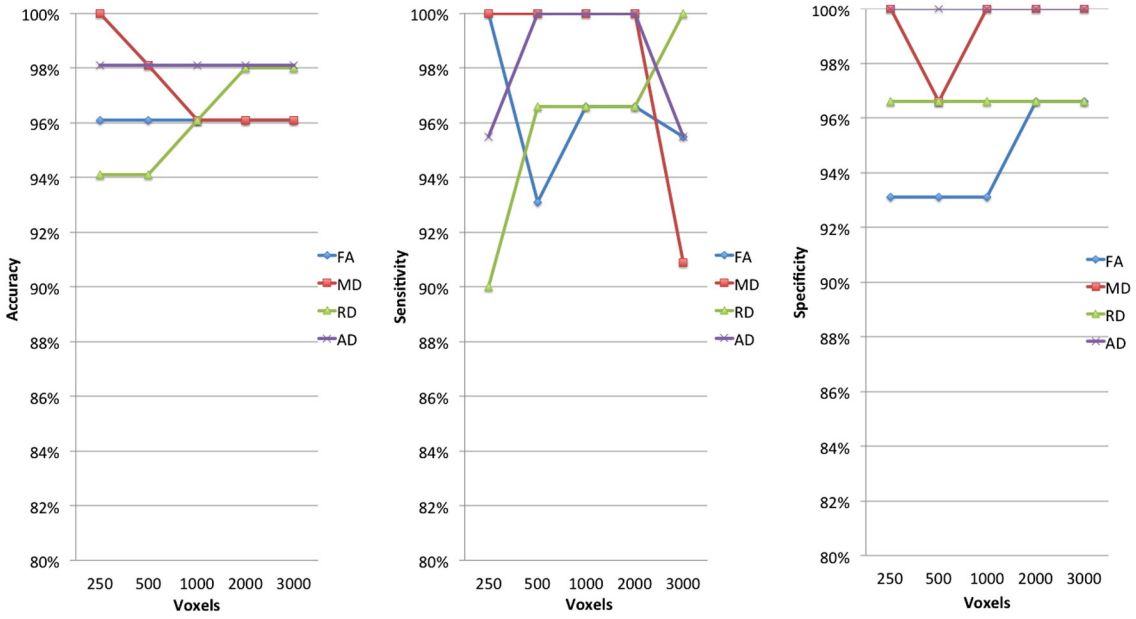

Fig. 4. Accuracy, sensitivity and specificity for controls and epilepsy classification. The percent values reported are of the weighted average of the 10 cross-validation of the two classes, i.e. controls and children with epilepsy. The reported results are of the five reduced data sets — 250 voxel, 500 voxels, 1000 voxels, 2000 voxels and 3000 voxels. The reduced data sets were selected by the relief feature selection algorithm.

lateralization related epilepsy) as predictors of seizure remission (Berg et al., 2001a,b; Geelhoed et al., 2005; MacDonald et al., 2000). Remission rate varies markedly by epilepsy syndrome, an observation that is especially true for childhood-onset epilepsy (Berg et al., 2001a,b; Geerts et al., 2010; Mohanraj and Brodie, 2005). However, diagnosis of an epilepsy syndrome does not always provide reliable information about long-term prognosis. One concern is that syndrome diagnosis is sometimes made only later in a patient's course, at which time the outcome is essentially known (Bouma et al., 1997). Furthermore, other studies have reported that clinical factors have little influence on seizure remission (Camfield et al., 1996; Cockerell et al., 1995).

The mixed findings in the literature are likely due to methodological differences as to what constitutes a remission factor. One factor brain structure (specifically, cerebral white matter) may be an unbiased biomarker of seizure remission. However, to date differences in brain structures have been mainly used to characterize disparity for already

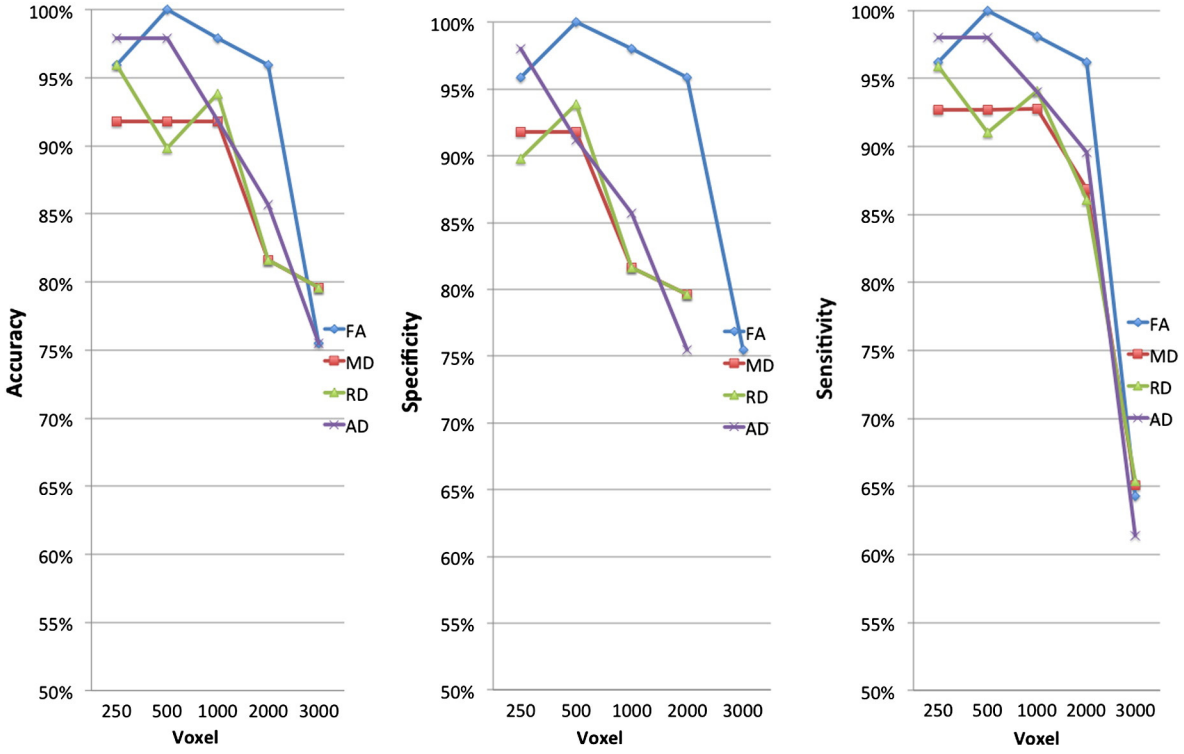

Fig. 5. Accuracy, sensitivity and specificity for controls, children with active epilepsy and children with remitted classification. The percent values reported are of the weighted average of the 10 cross-validation of the two classes, i.e. controls and children with epilepsy. The reported results are of the five reduced data sets — 250 voxel, 500 voxels, 1000 voxels, 2000 voxels and 3000 voxels. The reduced data sets were selected by the relief feature selection algorithm.

classified groups, i.e., controls vs. epilepsy groups. Hence, information that may guide treatment and perhaps differentiate seizure remission from intractable seizures requires the ability to distinguish brain structures within the epilepsy group at the time of diagnosis. This is an important direction for future research. Our prior study was among the first to characterize white matter differences between children with active epilepsy and those with remitted epilepsy 5–6 years after seizure onset (Amarreh et al., 2013). Furthermore, our results show that an SVM can correctly identify children with active epilepsy with a high degree of accuracy in this preliminary investigation (100% with FA).

Most MRI-based SVM studies have used two-group comparisons. This approach results in a binary classification with 50% accuracy by chance alone. Also, this scenario is artificial to a certain extent since in clinical practice the potential options are usually not binary but will include several distinct possibilities. The three-way SVM classification (controls versus children with active epilepsy versus children with remitted epilepsy) therefore constitutes a more realistic setting. Additionally the chance accuracy of such a 3-way classification decreases to 33.3%.

There are several limitations to our study. First, the sample size was small, and investigation of a larger sample will prove to be most helpful in determining the reliability of the present findings. The small sample size resulted in children with heterogeneous seizure syndromes being grouped together for analysis, which likely obscured potential important findings unique to specific syndromes. Larger sample sizes will provide more reliable and stable indicators of classification accuracy. Second, all 9 subjects in the active group remained on anti-epileptic drugs (AEDs); in contrast, no subject in the remitted group was on AEDs. Therefore, the present findings should be interpreted cautiously in light of the small size and medication differences. While clinically the aim is to distinguish between seizure remissions from intractable seizures near the onset of epilepsy, such analysis is not possible in the current cohort; a longitudinal study using machine-learning methodology outlined here is planned for future research.

5. Conclusion

In summary, the observed white matter differences and the success of SVM classification in childhood epilepsy are encouraging and suggest the potential use of the SVM classification as a novel and automated approach to generate an early indicator of epilepsy course. This study showed that SVM method is sensitive to the WM structural differences between (i) controls and children with epilepsy and (ii) children with active epilepsy and children with remitted epilepsy. DTI-based SVM classification appears promising as a prognostic and diagnostic tool. However, further studies are needed to evaluate the diagnostic power in this context and to replicate our findings in different cohorts. Additionally, longitudinal studies are needed in order to develop an SVM classifier as a prognostic tool. Finally, SVM classification based on multiple contrasts or imaging modalities, such as functional data from fMRI, would be an interesting direction for the future as well.

Acknowledgments

All phases of this study were supported by NINDS 3RO1-44351 and by the Clinical and Translational Science Award (CTSA) program through the NIH Center for Advancing Translational Sciences (NCATS), grant UL1TR000427. The funding source was not involved in study design, data collection, analysis or manuscript preparation. We thank Raj Sheth MD and Monica Koehn MD for study participation and subject recruitment. Also greatly appreciated are Dace Almane, Melissa Hanson, Kate Young, and Bjorn Hanson for overall study coordination, participant recruitment, cognitive assessment, and data management.

We thank all subjects for participating in the study. We also thank Dr. Stefano Diciotti and Dr. Laurence O'Dwyer for providing the MATLAB codes used in the SVM analysis.

Appendix A. Supplementary data

Supplementary data to this article can be found online at http://dx.doi.org/10.1016/j.nicl.2014.02.006.

References

Amarreh, I., Dabbs, K., Jackson, D.C., Jones, J.E., Meyerand, M.E., Stafstrom, C.E., et al., 2013. Cerebral white matter integrity in children with active versus remitted epilepsy 5 years after diagnosis. Epilepsy Res. 107 (3), 263–271.

Arfanakis, K., Hermann, B.P., Rogers, B.P., Carew, J.D., Seidenberg, M., Meyerand, M.E., 2002. Diffusion tensor MRI in temporal lobe epilepsy. Magn. Reson. Imaging 20 (7), 511–519.

Berg, A.T., Shinnar, S., Levy, S.R., Testa, F.M., Smith-Rapaport, S., Beckerman, B., 2001a. Early development of intractable epilepsy in children: a prospective study. Neurology 56 (11), 1445–1452.

Berg, A.T., Shinnar, S., Levy, S.R., Testa, F.M., Smith-Rapaport, S., Beckerman, B., et al., 2001b. Two-year remission and subsequent relapse in children with newly diagnosed epilepsy. Epilepsia 42 (12), 1553–1562.

Bouma, P.A., Bovenkerk, A.C., Westendorp, R.G., Brouwer, O.F., 1997. The course of benign partial epilepsy of childhood with centrotemporal spikes: a meta-analysis. Neurology 48 (2), 430–437.

Camfield, C., Camfield, P., Gordon, K., Dooley, J., 1996. Does the number of seizures before treatment influence ease of control or remission of childhood epilepsy? Not if the number is 10 or less. Neurology 46 (1), 41–44.

Cockerell, O.C., Johnson, A.L., Sander, J.W., Hart, Y.M., Shorvon, S.D., 1995. Remission of epilepsy: results from the National General Practice Study of Epilepsy. Lancet 346 (8968), 140–144.

Concha, L., Beaulieu, C., Collins, D.L., Gross, D.W., 2009. White-matter diffusion abnormalities in temporal-lobe epilepsy with and without mesial temporal sclerosis. J. Neurol. Neurosurg. Psychiatry 80 (3), 312–319.

Desikan, R.S., Cabral, H.J., Hess, C.P., Dillon, W.P., Glastonbury, C.M., Weiner, M.W., et al., 2009. Automated MRI measures identify individuals with mild cognitive impairment and Alzheimer's disease. Brain 132 (8), 2048–2057.

Diehl, B., Busch, R.M., Duncan, J.S., Piao, Z., Tkach, J., Lüders, H.O., 2008. Abnormalities in diffusion tensor imaging of the uncinate fasciculus relate to reduced memory in temporal lobe epilepsy. Epilepsia 49 (8), 1409–1418.

Duncan, J.S., 2002. Neuroimaging methods to evaluate the etiology and consequences of epilepsy. Epilepsy Res. 50 (1–2), 131–140.

Duncan, J.S., 2008. Imaging the brain's highways-diffusion tensor imaging in epilepsy. Epilepsy Curr. Am. Epilepsy Soc. 8 (4), 85–89.

Fan, Y., Resnick, S.M., Wu, X., Davatzikos, C., 2008. Structural and functional biomarkers of prodromal Alzheimer's disease: a high-dimensional pattern classification study. NeuroImage 41 (2), 277.

Focke, N.K., Yogarajah, M., Symms, M.R., Gruber, O., Paulus, W., Duncan, J.S., 2012. Automated MR image classification in temporal lobe epilepsy. NeuroImage 59 (1), 356–362.

Geelhoed, M., Boerrigter, A.O., Camfield, P., Geerts, A.T., Arts, W., Smith, B., et al., 2005. The accuracy of outcome prediction models for childhood-onset epilepsy. Epilepsia 46 (9), 1526–1532.

Geerts, A., Arts, W.F., Stroink, H., Peeters, E., Brouwer, O., Peters, B., et al., 2010. Course and outcome of childhood epilepsy: a 15-year follow-up of the Dutch Study of Epilepsy in Childhood. Epilepsia 51 (7), 1189–1197.

Govindan, R.M., Makki, M.I., Sundaram, S.K., Juhász, C., Chugani, H.T., 2008. Diffusion tensor analysis of temporal and extra-temporal lobe tracts in temporal lobe epilepsy. Epilepsy Res. 80 (1), 30–41.

Hermann, B., Jones, J., Sheth, R., Dow, C., Koehn, M., Seidenberg, M., 2006. Children with new-onset epilepsy: neuropsychological status and brain structure. Brain 129 (10), 2609–2619.

Hutchinson, E., Pulsipher, D., Dabbs, K., Gutierrez, A.M., Sheth, R., Jones, J., et al., 2010. Children with new-onset epilepsy exhibit diffusion abnormalities in cerebral white matter in the absence of volumetric differences. Epilepsy Res. 88 (2–3), 208–214.

Kimiwada, T., Juhász, C., Makki, M., Muzik, O., Chugani, D.C., Asano, E., et al., 2006. Hippocampal and thalamic diffusion abnormalities in children with temporal lobe epilepsy. Epilepsia 47 (1), 167–175.

Klöppel, S., Stonnington, C.M., Chu, C., Draganski, B., Scahill, R.I., Rohrer, J.D., et al., 2008. Automatic classification of MR scans in Alzheimer's disease. Brain 131 (3), 681–689.

Knake, S., Salat, D.H., Halgren, E., Halko, M.A., Greve, D.N., Grant, P.E., 2009. Changes in white matter microstructure in patients with TLE and hippocampal sclerosis. Epileptic Disord. 11 (3), 244–250.

Koay, C.G., Chang, L.-C., Carew, J.D., Pierpaoli, C., Basser, P.J., 2006. A unifying theoretical and algorithmic framework for least squares methods of estimation in diffusion tensor imaging. J. Magn. Reson. 182 (1), 115.

Lemm, S., Blankertz, B., Dickhaus, T., Müller, K.R., 2011. Introduction to machine learning for brain imaging. NeuroImage 56 (2), 387–399.

MacDonald, B.K., Johnson, A.L., Goodridge, D.M., Cockerell, O.C., Sander, J.W.A.S., Shorvon, S.D., 2000. Factors predicting prognosis of epilepsy after presentation with seizures. Ann. Neurol. 48 (6), 833–841.

Magnin, B., Mesrob, L., Kinkingnéhun, S., Pélégrini-Issac, M., Colliot, O., Sarazin, M., et al., 2009. Support Vector Machine-based Classification of Alzheimer's Disease from Whole-brain Anatomical MRI, vol. 51. Springer, Berlin/Heidelberg pp. 73–83.

Meng, L., Xiang, J., Kotecha, R., Rose, D., Zhao, H., Zhao, D., et al., 2010. White matter abnormalities in children and adolescents with temporal lobe epilepsy. Magn. Reson. Imaging 28 (9), 1290–1298.

Mohanraj, R., Brodie, M.J., 2005. Outcomes in newly diagnosed localization-related epilepsies. Seizure 14 (5), 318–323.

Noble, W.S., 2006. What is a support vector machine? Nat. Biotechnol. 24 (12), 1565–1567.

Obenaus, A., Jacobs, R.E., 2007. Magnetic resonance imaging of functional anatomy: use for small animal epilepsy models. Epilepsia 48, 11–17.

O'Dwyer, L., Lamberton, F., Bokde, A.L., Ewers, M., Faluyi, Y.O., Tanner, C., et al., 2012. Using support vector machines with multiple indices of diffusion for automated classification of mild cognitive impairment. PLoS One 7 (2), e32441.

Orrù, G., Pettersson-Yeo, W., Marquand, A.F., Sartori, G., Mechelli, A., 2012. Using support vector machine to identify imaging biomarkers of neurological and psychiatric disease: a critical review. Neurosci. Biobehav. Rev. 36 (4), 1140–1152.

Platt, J., 1998. Sequential Minimal Optimization: A Fast Algorithm for Training Support Vector Machines: Microsoft Research.

Robnik-Šikonja, M., Kononenko, I., 2003. Theoretical and empirical analysis of ReliefF and RReliefF. Mach. Learn. 53 (1), 23–69.

Rodrigo, S., Oppenheim, C., Chassoux, F., Golestani, N., Cointepas, Y., Poupon, C., et al., 2007. Uncinate Fasciculus Fiber Tracking in Mesial Temporal Lobe Epilepsy. Initial Findings, vol. 17. Springer, Berlin/Heidelberg pp. 1663–1668.

Scholkopf, B., Sung, K.K., Burges, C.J.C., Girosi, F., Niyogi, P., Poggio, T., et al., 1997. Comparing support vector machines with Gaussian kernels to radial basis function classifiers. IEEE Trans. Signal Process. 45 (11), 2758–2765.

Shoeb, A., Edwards, H., Connolly, J., Bourgeois, B., Treves, S.T., Guttag, J., 2004. Patient-specific seizure onset detection. Epilepsy Behav. 5 (4), 483.

Smith, S.M., Jenkinson, M., Johansen-Berg, H., Rueckert, D., Nichols, T.E., Mackay, C.E., et al., 2006. Tract-based spatial statistics: voxelwise analysis of multi-subject diffusion data. NeuroImage 31 (4), 1487–1505.

Temko, A., Thomas, E., Marnane, W., Lightbody, G., Boylan, G.B., 2011. Performance assessment for EEG-based neonatal seizure detectors. Clin. Neurophysiol. 122 (3), 474.

Thivard, L., Lehéricy, S., Krainik, A., Adam, C., Dormont, D., Chiras, J., et al., 2005. Diffusion tensor imaging in medial temporal lobe epilepsy with hippocampal sclerosis. NeuroImage 28 (3), 682–690.

Trevor, H., Robert, T., 1998. Classification by pairwise coupling. Paper Presented at the Proceedings of the 1997 Conference on, Advances in Neural Information Processing Systems, 10.

Vapnik, V., Lerner, A., 1963. Pattern recognition using generalized portrait method. Autom. Rem. Contr. 24, 774–780.

Woolrich, M.W., Jbabdi, S., Patenaude, B., Chappell, M., Makni, S., Behrens, T., et al., 2009. Bayesian analysis of neuroimaging data in FSL. NeuroImage 45 (1 Suppl.), S173–S186.

World Medical Organization, 1996. Declaration of Helsinki. Br. Med. J. 313 (7070), 1448–1449.